Resources, Conservation & Recycling 198 (2023) 107174

Contents lists available at ScienceDirect

Resources, Conservation & Recycling

journal homepage: www.elsevier.com/locate/resconrec

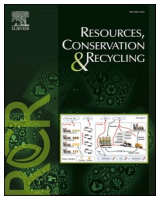

Full length article

Sodium oxalate activation of basic oxygen furnace slag for building materials

Winnie Franco Santos [a,*], Jan-Joost Botterweg [a,*], Stefan Chaves Figueiredo [a], Katrin Schollbach [a], Sieger van der Laan [a,b], H.J.H. Brouwers [a]

[a] Department of the Built Environment, Eindhoven University of Technology, P.O. Box 513, 5600 MB Eindhoven, the Netherlands
[b] Tata Steel, R&D, Microstructure & Surface Characterization (MSC), P.O. Box 10.000, 1970 CA IJmuiden, the Netherlands

ARTICLE INFO

Keywords:
Steel slag
Chemical activation
Ca-oxalate
Value-added recycling
Heavy metals

ABSTRACT

Basic oxygen furnace (BOF) slag is a waste from the steel-making process characterised by its low hydraulic behaviour and heavy metals content. This study investigates activation of BOF slag with disodium oxalate to enhance the early hydration kinetics, microstructure development and heavy metals retention to develop it as a 100% replacement alternative for ordinary Portland cement. The results reveal that the activator boosts the reactivity not only of brownmillerite and calcium silicate but also Mg-wuestite. The main products formed are hydrogarnets and calcium-silicate-hydrate (C-S-H) gel. The maximum dosage added of 3 wt.% reached sufficient strength of 32.8 MPa at 28 days, being the most promising mixture. Leaching results of heavy metals are below the Dutch Soil Quality Decree limits. In summary, the BOF slag-oxalate cement offers an attractive approach for the future of steel-making and the building materials industry.

1. Introduction

Basic oxygen furnace (BOF) slag is a solid waste from the steel-making process route, also referred to as converter steel slag, annually produced in high quantities. The world crude steel production reached 1951 million tons in 2021, from which, around 246 million tons of BOF slag were generated, during the refinement of pig iron to raw steel (World Steel Association, 2022). Different from blast furnace slag, which is already used in blended cements for construction materials (Scrivener et al., 2018), BOF slags are not yet inserted in the market as a high-value product, since there are usually barriers such as low hydraulic properties. In the US and European countries, 60–70% of BOF slag can be recovered and used in low-end applications as aggregate in concrete or backfill materials, whereas in other countries this range varies between 20 and 25% (Jiang et al., 2018; Song et al., 2021). The majority of the BOF slag is landfilled or stockpiled, occupying land resources and leading to potential environmental pollution due to leachates from the slag.

Increasingly strict legislations and CO_2 emissions targets to reduce the environmental impact, stated by the Intergovernmental Panel on Climate Change (IPCC 2019), drive industrial parks around the world to develop technological innovation towards implementing green upgrading and circular economy (Habert et al., 2020). After water, concrete is the most used material across the globe, usually composed of ordinary Portland cement (OPC) as a binder. The increased demand for OPC production could lead to 10% of total anthropogenic CO_2 emissions in the near future (Monteiro et al., 2017; Miller et al., 2018). For that reason, alternative binders are needed to meet the global demand for concrete and the emissions goals. Therefore, valorising and promoting BOF slag as a binder could reduce environmental impacts.

BOF slag has been researched with intense interest (Shi, 2004; Liu and Guo, 2018; Yi et al., 2012; Wang et al., 2010; Wang et al., 2022; Ahmed et al., 2023; Zepper et al., 2023). It has potential as a cementitious material regarding its similarity to OPC in composition and mineralogy. The BOF slag contains as main phases the α`- and β- polymorphs of dicalcium silicate Ca_2SiO_4 (C_2S) (Belhadj et al., 2012), brownmillerite ($Ca_2(Fe, Al)_2O_5$) (van Hoek et al., 2016) and wuestite (Fe, Mg)O (Monteiro et al., 2017). Replacing 5–20% of OPC with BOF slag is possible without compromising the material properties. However, at higher replacements, besides the low reactivity of the slag, it delays the hydration process, leading to a decrease in strength development. One material inhibits the hydration of the other, the OPC restricting the hydration of the BOF slag phase brownmillerite and the BOF slag decreasing the ettringite and calcium silicate hydrate formation in OPC

* Corresponding authors.
E-mail addresses: w.franco.santos@tue.nl (W. Franco Santos), janjoostbotterweg@gmail.com (J.-J. Botterweg).

https://doi.org/10.1016/j.resconrec.2023.107174
Received 22 January 2023; Received in revised form 12 August 2023; Accepted 13 August 2023
Available online 16 August 2023

(Shi, 2004; Liu and Guo, 2018; Yi et al., 2012). It is also reported that BOF can cause environmental problems with the leaching of vanadium (V_2O_5) (van Zomeren et al., 2011) and chromium (Cr_2O_3) (Chaurand et al., 2006; Pan et al., 2017; Jiang et al., 2018). Consequently, its application is still limited, failing to make full use of its cementitious properties.

Alkali activators are commonly used to enhance the reactivity of aluminosilicate precursors like fly ash and ground blast furnace slag (GBFS) to produce geopolymers (Provis and van Deventer, 2009; Provis, 2018). Many researchers have accelerated the hydration of BOF slag using chemical activators such as NaOH, NaCl, $NaCO_3$, Na_2SO_4, N $(CH_2CH_2OH)_3$ (triethanolamine) known as TEA and $C_9H_{21}NO_3$ (tri-iso-propanolamine) known as TIPA (Belhadj et al., 2012; Zhao et al., 2017; Shi and Qian, 2000; Salman et al., 2015; Cristelo et al., 2019). However, BOF slag is a Fe- and Ca-rich material with low alumina and silica content and will not form an aluminosilicate gel as in geopolymers. Applying conventional alkali activators in pure BOF slag can initiate the early reaction of C_2S, although it has little influence on hydration at later ages (after 7 days) (Wang et al., 2012). They will develop the compressive strength of BOF slag only to a range of 16–25 MPa after 28 days of hydration (Belhadj et al., 2012; Zhao et al., 2017; Shi and Qian, 2000; Salman et al., 2015; Cristelo et al., 2019), below the minimum value (32.5 MPa) described by the European standard (BS EN 197-1, 2011). Therefore, a suitable activator for BOF slag should promote the dissolution of the Ca- and Fe-bearing phases.

Alahrache et al. (2016) investigated the effect of sodium oxalate in fly ash-OPC blends. They found that the addition of sodium oxalate consumed portlandite and calcium by the precipitation of stable complexes of calcium oxalate. In solutions saturated with Ca^{2+}, oxalates form a thermodynamically stable phase of calcium oxalate monohydrate ($CaC_2O_4.H_2O$) called whewellite. In addition, the formation of $CaC_2O_4.H_2O$ can modify mechanical properties and durability by decreasing porosity and permeability since it disperses on the surface and fills up pores forming a protective layer against corrosion and exposition to chemical weathering (Singh et al., 2003; Zhang et al., 2021) because of the low solubility (Burgos-Cara et al., 2017). In OPC blends, the organic compound oxalate can also work as a superplasticiser reducing the water demand of the mixture and as an activator enhancing early hydration (Manuel and Cobos, 2018).

In nature, certain living organisms (plants) produce oxalate to form strong bonds with heavy metal ions for detoxication purposes. It is an organic conjugated base that has a low molecular weight and carries the function of oxygen donor in metal-ligands, due to its ability to chelate heavy metals (Osmolovskaya et al., 2018). The same principle is used in industrial applications, as oxalate is a common chelating agent applied to remediate metals. Large organic molecules covalently bond with metal ions to form a stable complex (Spence and Shi, 2005), therefore could immobilise hazardous elements, like Vanadium and Chromium from the BOF slag.

The sodium salt is the cheapest amongst the soluble oxalates, and due to the composition with two carboxylate groups (COO^-), researchers are looking into methods to produce oxalates from the capture of atmospheric carbon dioxide (CO_2) (Paris and Bocarsly, 2019; Li et al., 2019; Schuler et al., 2022; Boor, 2020). Nevertheless, oxalates have limited application. The possibility of combining sodium oxalate with BOF slag could expand the application of oxalate and make use of the BOF slag as a stand-alone cementitious material. As far as found in literature, no research has been conducted on the quantification of the reaction products from BOF slag activated with low dosages of disodium oxalate as a precursor binder in building materials. Neither has the effect of this activation on the immobilisation of heavy metals been investigated.

In this paper, the effectiveness of disodium oxalate as a BOF slag activator, for Portland cement -free binder, is investigated. A multi-technique approach is carried out to explore the influence of the disodium oxalate dosage on the early and late-age hydration of BOF slag. The phase development, microstructural and mechanical properties of BOF slag pastes are investigated using quantitative XRD, thermogravimetric analysis, calorimetric measurements, mechanical performance testing and the setting behaviour of the mixes is discussed. In addition, leaching tests are carried out to evaluate the retention of heavy metals.

2. Materials and methods

2.1. Materials properties

The BOF slag is the only starting material used for this study. It was provided by Tata Steel (IJmuiden, The Netherlands). The BOF slag is produced in heats of ~30 tons during the refinement of 300 tons of hot metal and scrap to produce steel. After the refinement process, the BOF slag is poured into open pits, followed by secondary water cooling. A representative sampling of 1500 kg of representative production from a batch of ~200 BOF slag heats, was obtained in the 0–25 mm size fraction. Subsequently, this material was dried, sieved and crushed to below 5.6 mm. The slag was collected and then stored in air-tight plastic drums to prevent carbonation. The grinding procedure was performed using a Retsch RS 300 XL disc mill at a constant speed of 912 min^{-1} for 20 min and was selected for an input of 1 kg in a grinding jar volume of 2l

The elemental composition of the BOF slag was determined by X-ray fluorescence analysis (XRF) and reported as oxide percentages. The analysis was performed with an XRF spectrometer from PANalytical (Epsilon 3 range, standardless OMNIAN method), on a fused bead. The loss of ignition was evaluated beforehand by heating the sample to 1000 °C for 1 h. The chemical and physical composition of the BOF slag is given in Table 1. As expected, it is mainly composed of CaO, Fe_2O_3, SiO_2, MgO and MnO, while Al_2O_3, TiO_2, V_2O_5 and Cr_2O_3 are present as minor constituents. Note that valency states of the metal Fe, Mn, V and Cr have not been determined, and e.g., Fe-oxide is largely present in the divalent form. The contents of Fe_2O_3 and MgO are significantly higher than those in OPC, while CaO is lower. The specific surface area (SSA) of the BOF slag was measured by nitrogen adsorption (Tristar II 3020 V1.03 Series micrometre) using the Brunauer–Emmett–Teller (BET) method (Brunauer and Emmett, 1937), employing nitrogen at 77 K. The BOF slag density was measured with a Helium pycnometer (AccuPyc II 1340). The particle size distribution (PSD) was obtained by laser light scattering using the Malvern Mastersizer 2000® PSD analyser.

The activator, disodium oxalate ($C_2Na_2O_4$), was an industrial-grade material (Acros Organics®, extra pure - 98.5%- CAS number 62-76-0).

Table 1
Chemical and mineralogical composition and physical properties of the BOF slag.

Chemical composition		Phase composition		Physical properties	
Al_2O_3	3.92	Wuestite	28.9	ρ (g/cm^3)[a]	3.69
CaO	37.81	Magnetite	5.1	D_{10}(μm)[b]	0.99
Fe_2O_3	26.24	Brownmillerite	17.8	D_{50}(μm) [b]	8.82
MgO	5.77	C_2S (α'+β)	28.2	D_{90}(μm) [b]	39.39
MnO	4.42	Hatrurite	1.4	SSA_{BET} (m^2/g)[c]	2.02
P_2O_5	1.1	Lime	0.8		
SiO_2	10.97	Calcite	0.0		
TiO_2	1.36	Dolomite	1.2		
V_2O_5	0.91	Amorphous	16.7		
Cr_2O_3	0.28				
GOI	0.47				

Note: when BOF slag is heated in air to 1000 °C for loss of ignition, a mass gain (GOI) of 0.47wt% is induced due to the oxidation of metallic or divalent iron and manganese.

[a] Particle specific gravity from He pycnometer.

[b] D-values obtained by Laser diffraction granulometry.

[c] Specific surface area obtained by BET method.

2.2. Samples preparation

The materials used for the present study are pure BOF slag paste with di-sodium oxalate as an activator. The water/slag ratio (w/s) used was 0.18, the minimum ratio that enabled sufficient workability when mixing and casting the paste. The percentages of the activator investigated are 1, 2 and 3 wt.% of the BOF slag weight, based on preliminary tests (Botterweg, 2021) and previous publication by our research group with another strong conjugated base as an activator (Kaja et al., 2021a).

Before adding the BOF slag, the solution of activator and water was put in a dynamic shaker (ES-SM-30- Edmund Buhler GmbH) for 1 hour at a rate of 250 rotations per minute.

The pastes were mixed according to the EN196-1 (CEN 2008), cast in cubic moulds with the dimensions of 40 × 40 × 40 mm. Subsequently, they were stored at 20 °C, and RH of 60% sealed with parafilm and cured for 1,7,28 and 91 days. The samples were named based on the concentration of Na_2 -oxalate added: S100-X1, S100-X2 and S100-X3.

2.3. Methods

2.3.1. Hydration kinetics

The hydration kinetics were investigated in an isothermal calorimeter (TAM Air, Thermometric) at a constant temperature of 20 °C for 65 h. The solutions of activator with 1, 2 and 3% (by wt.% of slag) and water with a w/s ratio of 0.3 were adopted and put in a dynamic shaker (ES-SM-30- Edmund Buhler GmbH) for 1 h at a rate of 250 rotations per minute before adding to the BOF slag. The BOF slag was mixed with the solutions of water and Na_2 -oxalate in a glass ampule, homogenised in a vortex shaker for 1 min and placed right after in the calorimeter. For the hydration kinetics comparison, a reference (BOF slag) was prepared with only slag. Note that for the paste's cubes in this investigation, a w/s ratio of 0.18 was chosen owing to the water-reducing superplasticizing effect of the oxalate. The pH value of the Na_2 -oxalate solutions with water is measured with a Voltkraft PH-100ATC pH electrode.

2.3.2. Setting and mechanical properties

The initial and final setting time of the mixtures has been determined according to EN196-3 (CEN 2008) using the Vicat needle method at room temperature of around 20 °C (±5 °C). The compressive strength of the pastes for each composition was determined on the cubic samples (three replicates) using a loading rate of 2400 N/s according to EN196-1. Pastes were covered with foil and cured in the climate chamber (20 °C, RH > 95%) until the testing age.

2.3.3. Mineralogy of the slag and pastes

Quantitative X-ray diffractograms (QXRD) were measured using a Bruker D4 endeavor X-ray diffractometer, with Lynx Eye detector and Cobalt radiation Kα radiation (λ= 1.790 Å), with accelerating voltage 40 kV and current of 40 mA, a step size of 0.02° 2θ, for a 2θ range of 10–90° 2θ and fixed divergence slits of 0.5°

The phases were identified with the Bruker software DIFFRAC.EVA 4.3 using the ICDD PDF-2 database and quantified with the Bruker software Topas 4.2 (Coelho, 2018) by the Rietveld method (Gualtieri, 2000). For the quantification of the amorphous content, 10 wt.% of crystalline Si (XRD Silicon powder) was added to the samples as an internal standard and homogenised by grinding in the McCrone Retsch XRD mill for 20 min. All the Rietveld quantification analysis, 1 σ errors values, and corresponding statistical criteria Rwp (R-weighted-profile) and GOF (goodness-of-fit) (Toby, 2006; Post and Bish, 1989) of the measurements and the crystal structures codes of all the identified phases were taken from AMCS, ICSD or PDF database specified in Appendix A (Table A1, A2, A3, A4).

2.3.4. Thermogravimetric analysis

For thermogravimetric analysis (TGA/DTG), a Jupiter STA 449 F1 from Netzsch, was used with a heating rate of 10 °C/min in a continuous N_2 flow up to 1000 °C. The stepwise method was used for phase quantification. The amount of portlandite was quantified with a tangential method.

2.3.5. Hydration stoppage

For the quantitative XRD and thermogravimetric analysis, after compressive strength tests, the same samples with the 3 different dosages of Na_2-oxalate were crushed to a particle size of < 1 mm and ground in an agate mortar. Hydration stoppage was performed using the double solvent exchange method (Snellings et al., 2018) (15 min in isopropanol, flushing with diethyl ether, 8 min drying at 40 °C in a half vacuum condition). The samples are then stored in a vacuum desiccator with silica gel to prevent carbonation due to exposure to ambient air during measurement and measured one by one within 48 h after completing the solvent exchange procedure.

2.3.6. Degree of hydration

Measurements of the hydration-stopped samples powder were used to derive the degree of hydration of the anhydrous BOF slag phases. The degree of hydration of the BOF slag was determined at 1,7,28 and 91 days using a combination of XRD – Rietveld refinement and TGA bound water content determined based on the mass loss between 40 °C and 550 °C. To quantify the degree of hydration of the BOF slag and its components the quantification results were recalculated to the initial anhydrous BOF slag mass to enable comparison.

2.3.7. Environmental risks – leaching analysis

Leaching tests upon chemical-activated BOF slag, have been conducted at 24 h and 28-day cured pastes, following the European standard for one-stage batch leaching test (EN 12457-2, 2002). The samples were crushed and sieved below 4 mm. This material was placed in deionised water (0.055 uS/cm) in a liquid-to-solid ratio of 10 l/kg, and the mixture was homogenised in a dynamic shaker (ES-SM-30 by Edmund Buhler GmbH) for 24 h, vibrating at 250 rpm. After 24 h the leachate is filtered using a filter paper with a pore diameter of 5 μm from which two different samples are taken as explained below. The pH value of the leachate after the filtered sample is measured with a Voltkraft PH-100ATC pH electrode. From the first sample, a small quantity is taken and filtered by use of a syringe filter with a pore diameter of 0.22 μm (Whatman) and acidified by the addition of concentrated and ultra-pure Nitric acid (HNO_3). The leachate is analysed upon the content of heavy metals, such as Chromium (Cr)and Vanadium (V) by inductively coupled plasma optical emission spectrometry (ICP OES- Spectroblue) according to NEN 6966 (NEN-EN 6966, 2005). The obtained elements' concentrations were compared with the legal limits specified in the Dutch Soil Quality Decree (DSQD) (Dutch Government 2007).

3. Results

3.1. Effect of activator content on hydration kinetics

Isothermal calorimetry is deployed to investigate the reaction of the reference paste, composed of BOF slag and water, in comparison to the pastes of BOF slag containing 1, 2 and 3% of disodium oxalate (w/s of 0.3 for all samples). The results are shown in Fig. 1a. The heat is normalised by the mass of BOF slag in each sample. The BOF slag sample with only water does not exhibit any characteristic heat flow peak that could be allocated to its reaction phases. With the addition of 1wt% of oxalate (S100-X1), a heat flow maximum occurs after ~2 h. The additional increase in the sodium oxalate dosage led to the reduction of the peak intensity and the later start of the induction period. In the case of 2 wt.% of sodium oxalate, heat evolution occurs between 7 and 14 h followed by a second peak at ~20 h. In the case of 3wt% of sodium oxalate, the maximum heat release occurs at ~8 h. The cumulative hydration heat evolution curves are shown in Fig. 1b. With the increasing amount of sodium oxalate, the total heat released after 65 h of hydration

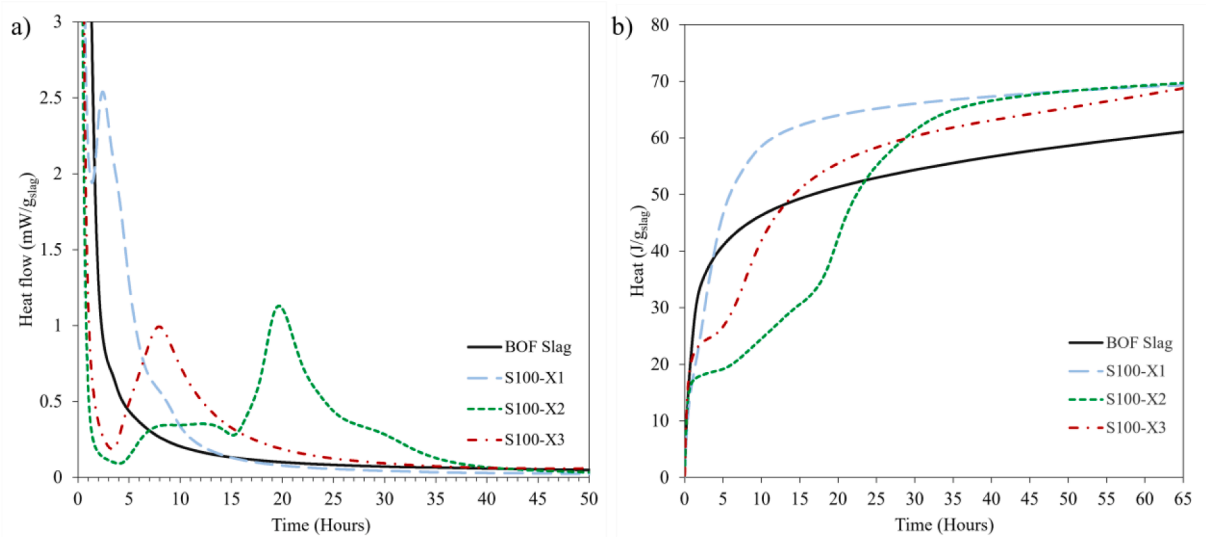

Fig. 1. a) Heat flow and b) cumulative heat evolution of BOF slag with dosages of disodium oxalate varying from 0 to 3 w.t.%. The w/*b* = 0.3 for all samples.

increases by 10 J/g$_{slag}$ (from 60 to 70 J/g$_{slag}$) for all the additions, showing similar cumulative heat for all the samples activated. To investigate the influence of the oxalate dosage on the reactive phases providing earlier heat release in S100-X1, the initial setting time and mineralogy of the samples were further analysed in the following sections of this study.

3.2. Influence of activator on fresh and mechanical properties

The compressive strength development for each BOF slag paste containing 1, 2 and 3% of disodium oxalate (w/s of 0.18 for all samples) is presented in Fig. 2. After 1 day of curing, the activator dosage does not lead to significant differences in the compressive strength. Nevertheless, after the first 7 days, a rise in compressive strength can be seen with increasing oxalate content. The effect remains over the whole measurement timespan, where the S100-X3 mixture presents the highest compressive strength values out of the three oxalate additions with maximum strengths reaching 10, 26.7, 32.8, and 37.4 MPa at 1,7,28 and 91 days, respectively. Despite the significant increase in the strength of the activated BOF pastes after adding the sodium oxalate, further addition of the activator delays the setting (Fig. 2) of the BOF slag. For every 1wt% of disodium oxalate added, the initial setting time increases by 10 min. There is a gap of 50 min in between the initial and final

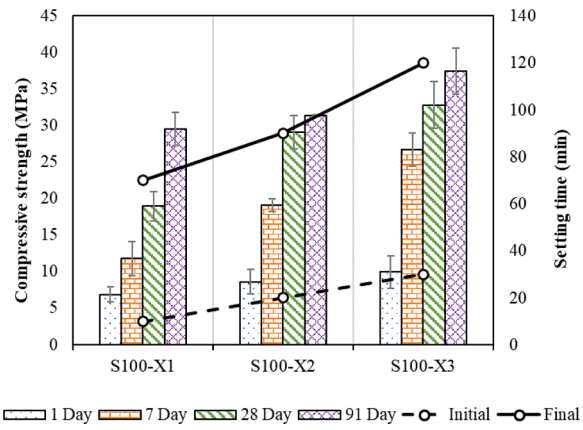

Fig. 2. Effect of the BOF slag with 1,2 and 3wt% of sodium oxalate on the initial and final setting time and compressive strength development.
Note: samples of BOF slag reference without oxalate did not develop sufficient strength to undergo the test.

setting time for S100-X1 and S100-X2. When the concentration of sodium oxalate increases further, this setting time gap is delayed to 60 min, as observed for S100-X3.

The oxalate dosage exerted varying influences on the setting and mechanical performance. As mentioned above (Section 3.1), the heat of hydration is positively correlated with the setting time, where S100-X1 will present its main reaction peak earlier than the other mixes, and S100-X2 reach its highest values of cumulative heat before S100-X3 (Fig. 1b). The activator decreased the viscosity of the suspension and improved its dispersion, giving workability retention to the mix, and behaving like an air-entraining agent (Taylor, 1997). It might also induce densification and strengthening effects of the material.

3.3. Reactive phases and contribution to the hydration

In order to evaluate which reactive phases contribute to the hydration of BOF slag, quantitative X-Ray diffraction (QXRD) analyses in samples after 1,7,28 and 91 days of hydration were investigated using the Rietveld method (Table A1- Appendix A). The major crystalline phases of BOF slag are wuestite, calcium silicate (C_2S) α' and β, brownmillerite (C_4AF), and magnetite. Wuestite is present in the BOF slag with different Mg and Fe contents, therefore two different crystal structures (Mg-rich and Fe-rich) were used for the refinement. The composition adopted for brownmillerite was $Ca_2Fe_{1.8}Al_{0.2}O_5$. Before hydration, the analysis also indicates the presence of amorphous phase with 16.7 wt.%. Fig. 3 shows the hydration evolution over time and the development of the new crystalline products in BOF slag-activated samples. Portlandite, hydrogarnets and pyroaurite were identified as crystalline reaction products.

A decrease in the wt.% of brownmillerite was observed for all concentrations of the activator after 24 h. The hydration of the brownmillerite phase is associated with the heat release observed during the first 5 h of hydration (Fig. 1a), because it is the only phase showing any significant reactivity after 1 day in sample S100-X1 (Table A1- Appendix A). It went from 17.8 to 13.2 wt.% on the first day of hydration with 1% of activator (Fig. 3a) and to 12 wt.% in samples S100-X3 (Fig. 3c), making it the most reactive phase at an early age, among the major BOF slag phases. The higher content of the activator (3%) played a major role in the rapidly hydrating brownmillerite phase. In contrast, the increased dosage of 3% of oxalate was slight to insignificant close to the 2 wt.% of activator (Fig. 3b) for the wuestite and C_2S hydration within day 1 of hydration. The dissolution of C_2S takes place beside the wuestite, which exhibits high reactivity in the presence of an activator, even higher than

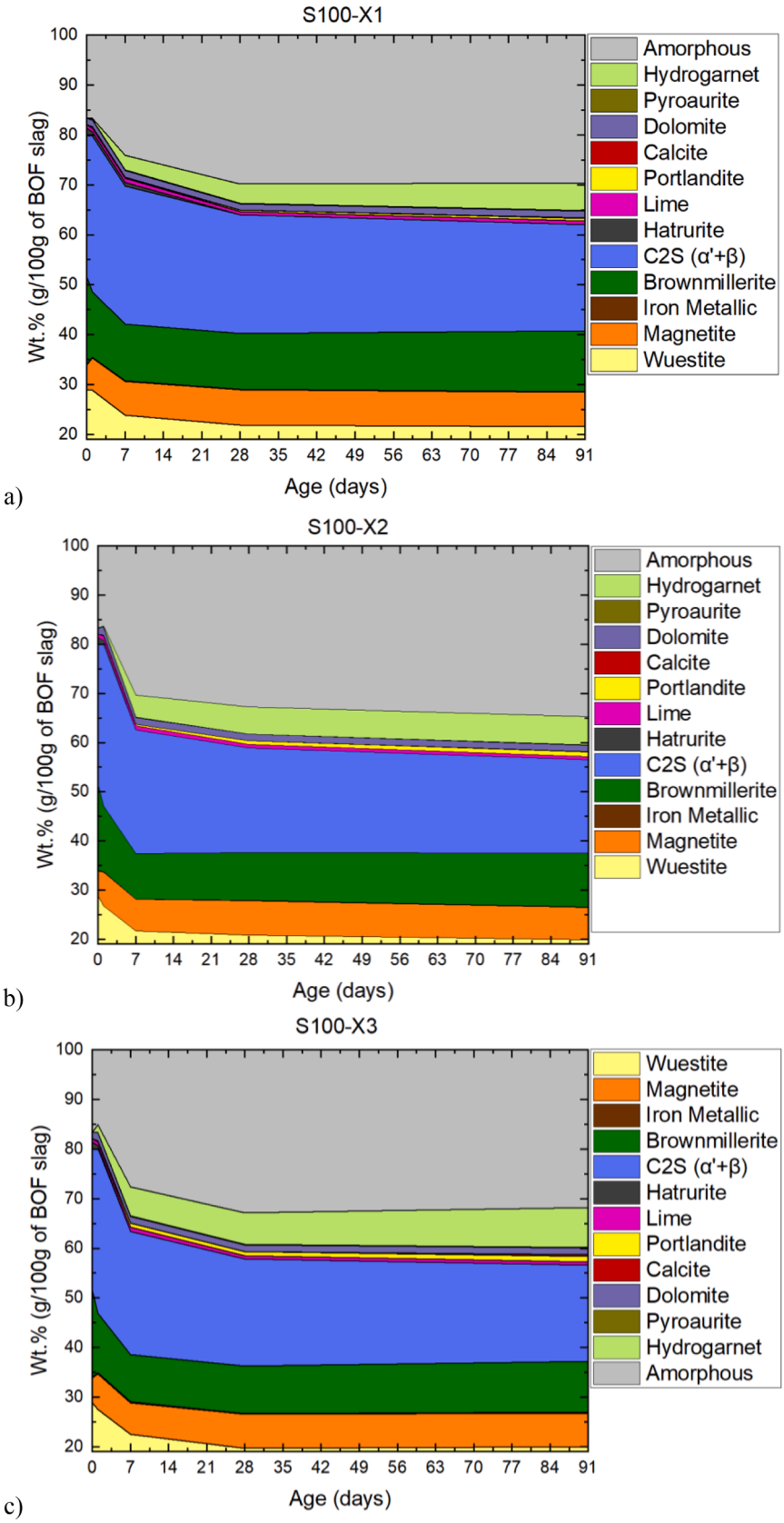

Fig. 3. Evolution of the individual BOF slag phase content over time during hydration for the different dosages of disodium oxalate a)1%, b)2% and c)3% measured by XRD- Rietveld analysis of hydration stopped powders.Note: the left axis Y scale starts in 20 w.t.% for a better resolution of the other phases. Colour should be used in print.

C_2S at an early age (Cuesta et al., 2021). With higher dosages than 1 wt. %, it was observed that the wuestite slightly contributes to the hydration of the slag within the first 24 h, though, after 7 days, the phase reduces from 28.9 to 23.8 wt.% with the lowest amount (1%) of activator. Also after 7 days, is when the dissolution of C_2S wt.% starts, presenting delayed hydration in comparison with the other main BOF phases, while with significant effect in comparison to other studies (Kaja et al., 2021a). The C_2S phase decreases from 28 wt.% to 24.8 wt% after 7 days (S100-X3), characterising its early hydration. and continued reacting over time.

As observed in the work of Kaja et al. (2021a), most of the brownmillerite hydration happens up to 7 days, influenced by the increase in the activator. However, in this study, the dosage of 2 or 3 wt.% of disodium oxalate does not influence the reactivity at later ages, presenting a similar hydration degree, that reaches up to 50 wt.%. The content of 2 or 3 wt.% of activator affects the reaction of the C_2S phases in such a similar pattern while with 1% of activator, the C_2S content does not decrease until 28 days, previously observed with other activators (Iliushchenko and Sedlă, 2022). The reactivity of the C_2S constantly increases over time, conversely to the other phases, for which the consumption was observed to slow down early on (like brownmillerite) or at later ages (wuestite). Literature (Kaja et al., 2021b) suggests that the hydration of C_2S in BOF slag plays a role in the durability improvement.

3.4. Hydration products formation

Fig. 4a shows the development of the crystalline products in BOF slag-activated samples. On 1 day of hydration, portlandite and hydrogarnets were identified as the crystalline products, increasing with evolution over time, both being directly proportional and influenced by the dosage of oxalate. However, in comparison with the hydrogarnet, the portlandite content detected for all ages is very low. The presence of pyroaurite was also revealed in the XRD analysis after 1 day of hydration, though in very small content. Rietveld analysis revealed that the hydrogarnet was the main crystalline hydration product in BOF slag as detailed reported before (Santos et al., 2023; Kaja et al., 2021a).

The addition of sodium oxalate results in the formation of new amorphous hydration phases as well (Fig. 4b). The dissolution of the amorphous phase occurs already within 24 h since the amorphous content wt.% decreases comparing S100-X3 to the other samples. The dosage of the oxalate did not exert the same influence in the new amorphous hydration products as in the crystalline hydrogarnets and portlandite. In the presence of water, C_2S hydrate forms calcium silicate hydrate (C-S-H) gel, contributing to the formation of amorphous hydration product C-S-H.

Together with brownmillerite, the amorphous content reacted rapidly at an early age (until 1 day). The findings evidence their role in the hydration kinetics and cause of the peaks observed in Fig. 1a. However, they respond differently to the different dosages of sodium oxalate added.

It was observed that the activator dosage does not influence the hydration qualitatively, as the same products are formed, but significantly changed the proportions of the major hydration products. Hydrogarnet formation reached its maximum value with 3% of disodium oxalate at 91 days of hydration with about 8 wt.%. Increased dosage of activator correlated well with higher content of hydrogarnet, the difference between 2 and 3% was established early on during the hydration. On the other hand, the dosage of 2% of the activator contributes to higher contents of amorphous hydration products.

Ramachandran showed the existence of calcium oxalate in cement containing oxalic acid and suggested that part of the strength development could be due to the formation of calcium oxalate during hydration (Ramachandran, 1972). Smillie disclosed the presence of calcium oxalate monohydrate when the oxalate concentration added to the cement mix was 10 wt.% (Smillie and Glasser, 1999). When adding oxalic acid to OPC, Singh et al. observed new reaction peaks in XRD after 91 days of hydration (Singh et al., 2003). Their new hydration phases were associated with the fast reaction of calcium aluminate and calcium ferrite but low reactivity with calcium silicates. In this current study, the slower reactivity of the activator with C_2S was also observed, taking place after 7 days of hydration. Up to 3 wt.% addition of the activator in BOF slag was not sufficient to identify oxalate-containing crystalline phase with XRDs in any period of observation until 90 days, owing to the low content of free lime and $Ca(OH)_2$ that could immediately bond with oxalate or due to the slow release of Ca^{2+} from the Ca-bearing phases.

Nevertheless, the XRD amorphous content doubles for all the activator dosages after the reactions already at 7 days (Fig. 3a–c) due to the amorphous nature of those oxalates/new hydration products that precede the formation of crystalline calcium oxalate (Ruiz-Agudo et al., 2017), which is a positive attribute to the reaction. Furthermore, the amorphous phase makes the material dense by filling in porosity, resulting in increased compressive strength (Singh et al., 2003). To further investigate the presence of calcium oxalate, the samples were analysed by thermogravimetry.

3.5. Thermogravimetric analysis and degree of hydration

TGA/DTG was applied to the samples containing 1–3 wt.% disodium

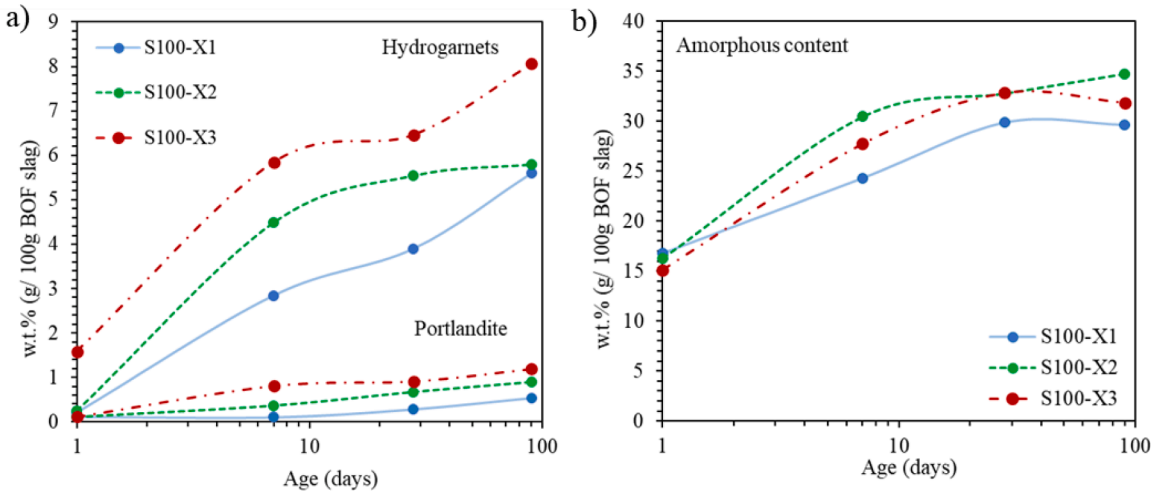

Fig. 4. The formation of (a) hydrogarnets and portlandite and (b) an increase in amorphous content over time for the different dosages of disodium oxalate determined by XRD- Rietveld analysis of hydration-stopped powders.

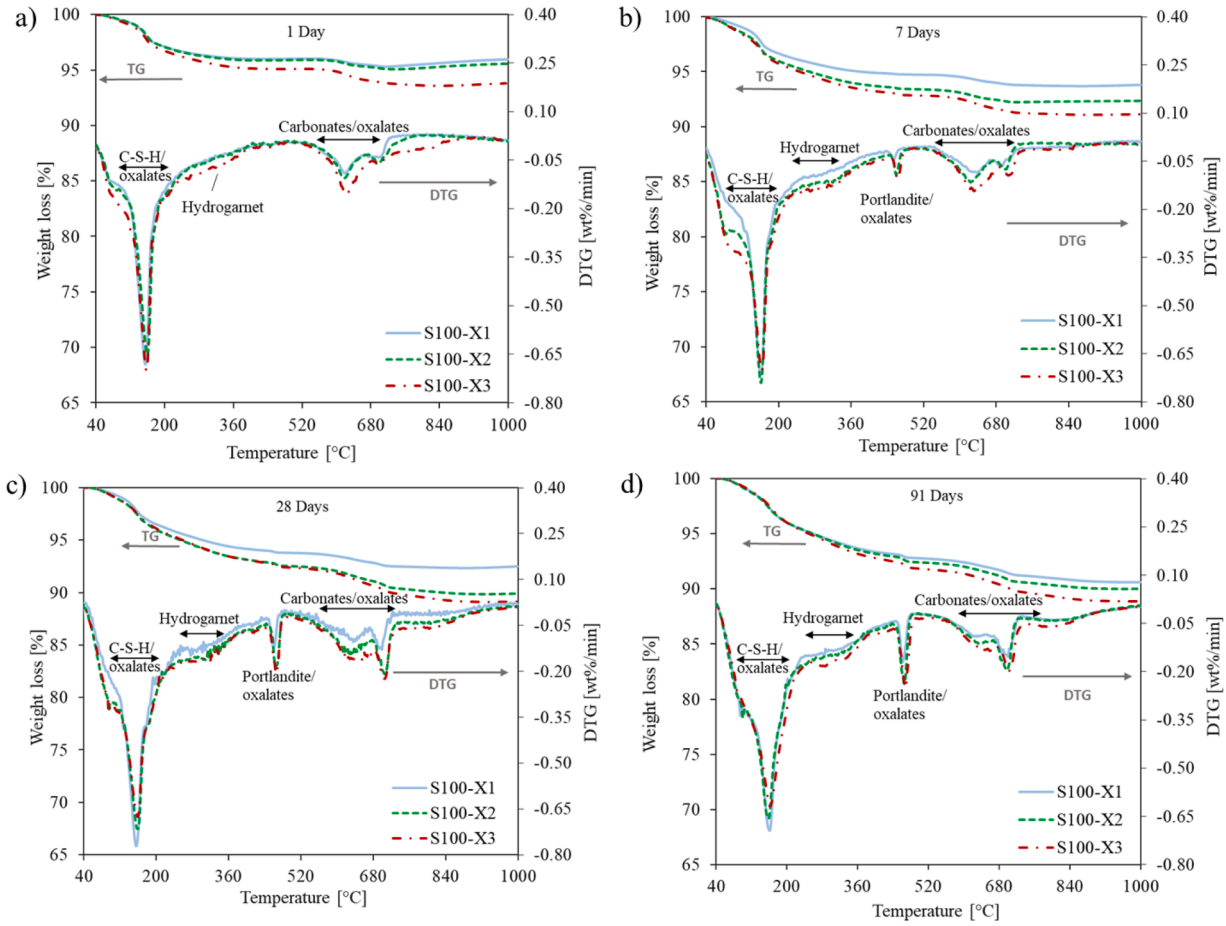

Fig. 5. Thermal analysis (TG and DTG) of BOF slag hydrated with 1,2 and 3 wt.% of disodium oxalate after a) 1, b) 7, c)28 and d)91 days.

oxalate (Fig. 5a–d). Thermogravimetric analysis shows that all samples over time show a significant amount of mass loss over the temperature range, from approximately 6 wt% at day 1 up to approximately 11 wt% at day 91. This mass loss is mainly due to the release of bound water, both physical and chemical within C-S-H and $Ca(OH)_2$, and of CO_2 within the $CaCO_3$.

The main mass loss due to water release from amorphous C-S-H gel occurs below 200 °C. The DTG confirms the findings in the XRD-Rietveld results of hydrogarnet formation after 1-day hydration with 3 wt.% disodium oxalate. The presence of hydrogarnet, portlandite and other hydration products was further confirmed by thermogravimetric analysis. The mass loss from hydrogarnet is assigned in the range between 200 and 360 °C (Dilnesa et al., 2013).

The amount of product formed before 200 °C after 1 day of hydration (Fig. 5a) is slightly higher for the activator dosage of 3 wt.%, whereas after 7 days starts being similar for all the samples. This observation diverges from the results measured of C_2S contribution with the XRD Rietveld method, suggesting that other reactions are happening, like the hydration of the amorphous C_2S that contributes to the formation of C—S—H gel. Crystalline oxalate phases could not be detected with XRD to support this. However, in the literature, there is evidence that calcium oxalate can precipitate via an amorphous precursor phase in an aqueous solution (Ihli et al., 2015). The early hydration of the amorphous content can explain the slow reaction of crystalline C_2S, when a high solution saturation is caused by the dissolution of the Ca-bearing phases, specially brownmillerite and other calcium silicates (Nicoleau et al., 2013) like the amorphous C_2S in the studied BOF slag (Santos et al., 2023).

A broad peak can be seen over the range of approximately 670–740 °C, generated by the decomposition of different carbonates, such as calcite ($CaCO_3$). Although calcite was not detected within the XRD analysis, the samples were carefully sealed and tested two days after hydration stoppage to avoid carbonation. The mass loss in this temperature range is intensified for every addition of disodium oxalate, showing that calcium oxalate compounds were formed in the system after 1 day of hydration and decomposed in a similar temperature range of C-S-H, portlandite and calcite.

Since calcium oxalate is used for calibration, it is known to show a characteristic sequence of phase changes upon heating (Lawson-wood and Robertson, 2016; Kloprogge, 2017), and its decomposition occurs in three different steps:

Overall decomposition reaction

$$CaC_2O_4.H_2O \rightarrow CaO+H_2O+CO+CO_2 \quad (1)$$

1 Dehydration around 115 °C

$$CaC_2O_4.H_2O \rightarrow CaC_2O_4+H_2O \quad (2)$$

2 Decomposition to calcium carbonate around 425 °C

$$CaC_2O_4 \rightarrow CaCO_3+CO \quad (3)$$

3 Decomposition to calcium oxide around 600 °C

$$CaCO_3 \rightarrow CaO+CO_2 \quad (4)$$

The initial spike in mass loss from 40 to 240 °C (Fig. 5a–d) can be

accounted for the dehydration of the C-S-H gel and calcium oxalate monohydrate ($CaC_2O_4.H_2O$). Afterwards, the mass loss that can be witnessed between 440 and 500 °C can be attributed to the presence of portlandite ($Ca(OH)_2$) releasing H_2O and calcium oxalate (CaC_2O_4) releasing CO (Eq. (3)).

The total BOF slag degree of reaction was calculated from the residual amounts of the primary phases at a given time compared to their initial amounts ($t = 0$) (Bizzozero, 2014; Lothenbach et al., 2016). The evolution of the BOF slag degree of reaction until 91 days is given in Fig. 6. BOF slag was found to react ~10% already on the first day of hydration and ~30% after 28 days with 3 wt.% of disodium activator. The effect of the addition of 1% of the activator dosage on BOF slag degree of hydration was observed to be limited in comparison with 2 and 3%. While the accelerating effect of the increase of activator dosage from 1 to 2% is clear, the results of the increase from 2 to 3% appear to be negligible at early ages, that the degree of hydration of both dosages overlaps from 1 to 90 days. Only at 28 days the dosages of 3% of activator slightly increase the degree of hydration in comparison with 2%. This behaviour happened because the 2 and 3 wt% added activator experiments both are performed with saturated solutions containing residual undissolved activator, while 1wt% is undersaturated with sodium oxalate.

The presence of crystalline calcite at the S100-X3 90d in a minimum amount (0.1) observed with QXRD (Table A1 in Appendix A) indicates that the natural carbonation of the sample hardly occurred, despite the possible amorphous nucleation of $CaCO_3$. Because of the strong bonds that the disodium oxalate makes with the chelated metals, will precipitate oxalates instead of carbonates (Chang et al., 2017). Is more likely that the Ca^{2+} from the $Ca(OH)_2$ quantified would bond to the oxalate present in the system, rather than carbonate, considering the small particle size of the slag samples, and the very low amount of water used, together with the compact structure of the hardened paste, (avoiding free spaces for porosity), preventing the CO_2 from entering naturally. Oxalate is known as a reducing agent, and although it is composed of C_2O_4, oxalate cannot form CO_3 at room temperature through an electrochemical reaction or be broken down to CO_2 without oxidoreductases (Anson and Stahl, 2020) or another reaction catalyser. On the other hand, calcite can participate in the dissolution reaction as a source of Ca ions for the precipitation of calcium oxalate monohydrate (Burgos-Cara et al., 2017). A similar explanation can be applied in the presence of dolomite (Zha et al., 2022).

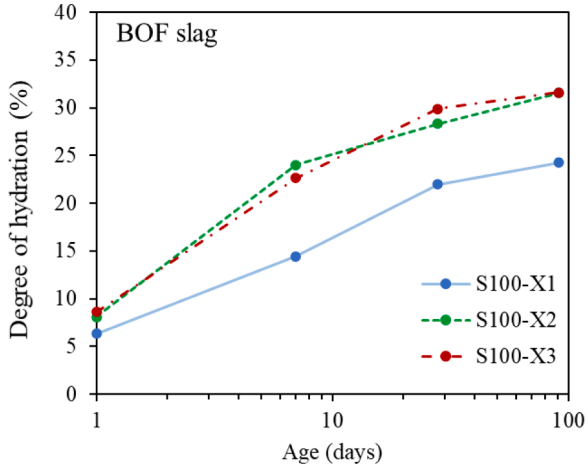

Fig. 6. Evolution over time of the degree of reaction of BOF slag during hydration at varying oxalate dosages. The data was derived by XRD-Rietveld analysis of hydration-stopped sample powders The amorphous content is not considered.

3.6. Environmental risks analysis

The presence of chromium (Cr) and vanadium (V) in the BOF slag composition suggest a possible risk of leaching heavy metals when applied as a building material. High leaching of V in BOF slag is commonly reported in the literature (van Zomeren et al., 2011; Cristelo et al., 2019). Therefore, the one-batch leaching test (EN 12457-2, 2002) was performed here to evaluate the capacity of the disodium oxalate activated samples to keep Cr and V retained in the hydration products after 1 and 28 days of hydration for each dosage of disodium oxalate. Table 2 compares the results to the legal limits set in the Dutch Soil Quality Decree (Dutch Government 2007) by the Dutch government and listed with their respective leachate pH values.

For the 1-day hydration, Cr leaching was well within the legal limits, while V was below the limit for samples S100-X1 and S100-X3 but surpassed in sample S100-X2 (2.1 mg/kg). After 28 days of curing, the V leaching decreased significantly compared to the 1-day results. Even in sample S100-X2, it is reduced to 0.21 mg/kg. In summary, after 28 days of hydration, all samples' leaching of Cr and V was reduced to far below the legal limits.

The distribution of heavy metals within the BOF slag phases affects the leaching behaviour of hydrated BOF slag. Cr is mostly incorporated in wuestite and brownmillerite, while V is in C_2S and brownmillerite. After hydration with water, Cr and V can be well immobilised by the hydration products, hydrogarnets and C—S—H gel (Santos et al., 2023). In this study, it is possible that after hydration, the V and Cr formed insoluble oxalates (Spence and Shi, 2005). In addition, the oxalate promoted the formation of new hydrated phases in a short time (1 to 7 days) by increasing the reactivity. These additional hydration products contribute to immobilising the heavy metals (Osmolovskaya et al., 2018; Bian et al., 2013), lowering the leaching.

The complexation with organic ligands and vanadate (V) can also occur at high pH, and the oxalate complexes, the vanadate (V), contribute to the mineral dissolution (Petter, 2019). They can form stable precipitates in a Ca-rich environment where the pH >12.5, like the samples in Table 2 with pH ranging from 12.8 to 13. The V is dependant on the dissolution of brownmillerite and C_2S, which accelerates at lower pH (van Zomeren et al., 2011).

The brownmillerite reacted to produce hydrogarnet, which is known to uptake Fe (Mancini et al., 2019), can take up Cr^{3+} as well (Kindness et al., 1994) and is weekly retained by calcium silicate (Moulin et al., 2000). The presence of portlandite in BOF slag contributes to the retention of the heavy metals in the amorphous hydration products. The heavy metals may be taken up by sorption onto the surface of the C-S-H or other ions` substitutions (Ahmed et al., 2022). Overall, the leaching results values do not present any restrictions on using oxalate activated BOF slag as a building material.

4. Discussion

Generally, oxalic acid acts as an accelerator in the hydration of OPC-based binders because its carboxylate ions strongly tend to form ionic bonds with the free lime and Ca-bearing phases to form calcium oxalate. The calcium oxalate is precipitated when oxalic acid is added to C_3S, and the concentration of Ca^{2+} ions close to the surface is kept low until all the acid is used up (Taylor, 1997). In the case of BOF slag, its Ca-bearing

Table 2
Leaching of inorganic contaminants measured by one stage batch leaching test after 1 and 28 days and the SQD legal limit values. All values in mg/kg.

ICP-Analysis	S100-X1		S100-X2		S100-X3		Legal Limits
Age	1d	28d	1d	28d	1d	28d	
pH	12.8	12.8	13.0	12.9	13.0	12.9	
Chromium (Cr)	0.09	0.01	0.14	0.02	0.14	0.01	0.63
Vanadium (V	1.02	0.18	2.1	0.21	1.49	0.19	1.8

phases CaO, $Ca(OH)_2$, Ca_2SiO_4 (C_2S) and brownmillerite ($Ca_2(Fe, Al)_2O_5$ release Ca^{2+} in the solution with the presence of Na_2-oxalate and water. The liberated Ca^{2+} can chelate with the oxalate, making more Ca^{2+} available in the solution. In the first stage of dissolution, CaO-bearing phases or free CaO participated, while the oxalate chelated the available Ca^{2+}. Moreover, if Mg is also liberated, it can bond with the oxalate, forming Mg-oxalates (Erdoğan et al., 2022). Considering the high dissolution of wuestite and the low amounts of crystalline pyroaurite detected with QXRD, it is likely that the Mg reacted with the oxalate.

Although in the quantification of the hydration products studies, there is not a bigger contribution between 2 and 3% after 7 days, the analysis shows that the increase in oxalate dosage promotes the compressive strength of the BOF slag pastes. The setting delay could result from the retarding effect in the hydration beginning process. Therefore, the retarding effect could be attributed to the prolonged dissolution of the Ca-bearing phases with the highest oxalate dosage. The early reaction of 1 day might have contributed to the strength development with the fast hydration of BOF slag phases brownmillerite and wuestite, as well as the higher formation of crystalline hydrogarnet (in the presence of C_2S) in 3%, enhancing the compressive strength. On the other hand, it can be suggested that the activator would fill more pores. Therefore, future investigation is needed on the influence of disodium oxalate on porosity.

According to the literature (Singh et al., 2003), the new reaction products of oxalate can also disperse inside the pores and seal the surface (Kapetanaki et al., 2020), benefiting the material by the densification of the microstructure. This could also influence leaching behaviour. Therefore, further investigation into the influence of disodium oxalate on microstructure and porosity should be considered when conducting long-term leaching studies.

Disodium oxalates are commonly used as reducing agents, therefore can change the valence state of Cr and its solubility. The reduction of Cr^{6+} in solution with oxalate needs further investigation.

5. Conclusions

This paper presents the first experimental research of a newly proposed cementitious binder that is Portland cement-free, prepared by reacting BOF slag with low dosages of disodium oxalate at room temperature, aiming to accelerate the initial hydration of BOF slag without compromising the later age strengths. The influence of the dosages of the activator on the leaching of heavy metals, setting time, strength development, reaction mechanisms and phase proportions were investigated. From this research, the following conclusions can be drawn:

On the first 24 h of hydration, the disodium oxalate boosts the dissolution of brownmillerite, being more reactive with the highest activator level of 3wt%. The brownmillerite presents a high degree of reaction, and its hydration probably explains the heat release peaks in the calorimeter in the first 24 h. The wuestite phase is accelerated in the presence of the activator at early ages as well. On the contrary, C_2S hydration was slow to insignificant before 7 days with the 1wt% dosage of activator. However, C_2S was the only BOF slag phase to show a continuous hydration pattern, showing its maximum at 91 days in the sample with 3 wt.% of disodium oxalate.

The main crystalline hydrates were hydrogarnet and portlandite. The amorphous hydrates observed with TGA were C-S-H and oxalate hydrates, more likely to be calcium oxalate. All primary slag phases contribute to the reaction, except for magnetite. The heavy metals Cr and V became partially immobilised in the new hydration products after 28 days.

The degree of hydration indicates that the reactions after 7 days with the dosage of 2 wt.% and 3 wt.% of disodium oxalate are very similar. Nevertheless, increasing oxalate dosages can effectively prolong the setting time and influence mechanical behaviour proportionally. The samples with 3 wt.% presents the longest initial setting time (30 min), and results in the highest compressive strength values at all ages, reaching 10, 26.7, 32.8, and 37.4 MPa at 1, 7, 28 and 91 days, respectively. The increased strength development proportional to activator dosage indicates that a continuous addition of oxalate could enhance the mechanical properties of the BOF slag mixes, although solubility should be considered.

In summary, the current study provides insight into the activation of BOF slag with low dosages (1–3 wt.%) of disodium oxalate as a potential binder in building material applications. Disodium oxalate acts as a superplasticiser and promotes strength development with increasing dosage. It reduces water demand and influences workability. The hydration products formed can retain the heavy metals, making the new proposed binder promising as an alternative cement in building materials. How the proposed binder responds to ambient carbonation is unknown and needs to be investigated in the future. As a continuation of the current research, assessing the long-term environmental risks and durability of oxalate activated BOF slag binder is recommended. An environment and carbon footprint assessment are suggested for developing and up-scaling the new binder. It would further the understanding of the potential and would narrow the remaining distance to the market for the proposed binder as a construction material.

The knowledge acquired in this research opens new approaches to reducing CO_2 emissions for the cement industry using BOF slag as a stand-alone cementitious material. It can be used to valorise BOF slag alone or as a replacement in cement and in combination with other by-products. It generates demand for the application of oxalates, especially those produced from capturing atmospheric CO_2, contributing to a sustainable society.

Data availability

The raw data required to reproduce these findings are available from the corresponding author upon request.

CRediT authorship contribution statement

Winnie Franco Santos: Conceptualization, Methodology, Investigation, Formal analysis, Writing – original draft, Writing – review & editing, Visualization, Supervision. **Jan-Joost Botterweg:** Investigation, Methodology, Data curation, Formal analysis. **Stefan Chaves Figueiredo:** Methodology, Visualization, Supervision. **Katrin Schollbach:** Methodology, Visualization, Writing – review & editing, Supervision. **Sieger van der Laan:** Resources, Writing – review & editing. **H. J.H. Brouwers:** Resources, Funding acquisition, Project administration.

Declaration of Competing Interest

The authors declare that they have no known competing financial interests or personal relationships that could have appeared to influence the work reported in this paper.

Data availability

Data will be made available on request.

Acknowledgements

The authors would like to acknowledge the financial support from NWO (The Netherlands Organization for Scientific Research) for funding this research (project no.10023338) and M2i (Materials Innovation Institute) for managing this project. Furthermore, the authors wish to express their gratitude to the following sponsors of this research: Tata Steel; ENCI; Hess AAC Systems; V.d. Bosch Beton.

Supplementary materials

Supplementary material associated with this article can be found, in the online version, at doi:10.1016/j.resconrec.2023.107174.

References

Ahmed, M.J., Cuijpers, R., Schollbach, K., Laan, S.v.d., Brouwers, H.J.H., 2022. V and Cr substitution in dicalcium silicate (C2S) under oxidizing and reducing conditions-Synthesis, reactivity, and leaching behaviour studies. J. Hazard. Mater. https://doi.org/10.1016/j.jhazmat.2022.130032.

Ahmed, M.J., Santos, W.F., Brouwers, H.J.H., 2023. Air granulated basic Oxygen furnace (BOF) slag application as a binder : effect on strength, volumetric stability, hydration study, and environmental risk. Constr. Build. Mater. 367, 130342 https://doi.org/10.1016/j.conbuildmat.2023.130342.

Alahrache, S., Winnefeld, F., Champenois, J.B., Hesselbarth, F., Lothenbach, B., 2016. Chemical activation of hybrid binders based on siliceous fly ash and Portland cement. Cem. Concr. Compos. 66, 10–23. https://doi.org/10.1016/j.cemconcomp.2015.11.003.

Anson, C.W., Stahl, S.S., 2020. Mediated fuel cells: soluble redox mediators and their applications to electrochemical reduction of O_2 and oxidation of H_2, alcohols, biomass, and complex fuels. Chem. Rev. 120, 3749–3786. https://doi.org/10.1021/acs.chemrev.9b00717.

Belhadj, E., Diliberto, C., Lecomte, A., 2012. Characterization and activation of Basic Oxygen Furnace slag. Cem. Concr. Compos. 34, 34–40. https://doi.org/10.1016/j.cemconcomp.2011.08.012.

Bian, M., Zhou, M., Sun, D., Li, C., 2013. Molecular approaches unravel the mechanism of acid soil tolerance in plants. Crop J. 1, 91–104. https://doi.org/10.1016/j.cj.2013.08.002.

Bizzozero, J., 2014. Hydration and Dimensional Stability of Calcium Aluminate Cement Based Systems, p. 6336.

Boor, V.S., 2020. Electrochemical Reduction of CO to Oxalic Acid Electrochemical Conversion, Down-Stream Processing and Techno-Economic Analysis. Delft University of Technology. http://repository.tudelft.nl/.

Botterweg, J., 2021. BOF Slag Composites For Extrusion-Based 3D Printing. Eindhoven University of Technology. https://doi.org/10.3390/app9091809.S.S.

Brunauer, S., Emmett, P.H., 1937. The use of low temperature van der waals adsorption isotherms in determining the surface areas of various adsorbents. J. Am. Chem. Soc. 59, 2682–2689. https://doi.org/10.1021/ja01291a060.

BS EN 197-1, 2011. Cement Part 1: Composition, Specifications and Conformity Criteria for Common Cements.

Burgos-Cara, A., Putnis, C.V., Ortega-Huertas, M., Ruiz-Agudo, E., 2017. Influence of pH and citrate on the formation of oxalate layers on calcite revealed by in situ nanoscale imaging. CrystEngComm 19, 3420–3429. https://doi.org/10.1039/c7ce00305f.

CEN, 2008. EN 196-3:2005+A1:2008 - Methods of Testing Cement - Part 3: Determination of Setting Times and Soundness.

Chang, R., Kim, S., Lee, S., Choi, S., Kim, M., Park, Y., 2017. Calcium carbonate precipitation for CO 2 storage and utilization: a review of the carbonate crystallization and polymorphism. Front. Energy Res. 5, 1–12. https://doi.org/10.3389/fenrg.2017.00017.

Chaurand, P., Rose, J., Domas, J., Bottero, J.Y., 2006. Speciation of Cr and V within BOF steel slag reused in road constructions. J. Geochemical Explor. https://doi.org/10.1016/j.gexplo.2005.08.006.

Coelho, A.A., 2018. TOPAS and TOPAS-Academic: an optimization program integrating computer algebra and crystallographic objects written in C++: An. J. Appl. Crystallogr. 51, 210–218. https://doi.org/10.1107/S1600576718000183.

Cristelo, N., Coelho, J., Miranda, T., Palomo, Á., Fernández-jiménez, A., 2019. Alkali activated composites – an innovative concept using iron and steel slag as both precursor and aggregate. Cem. Concr. Compos. 103, 11–21. https://doi.org/10.1016/j.cemconcomp.2019.04.024.

Cuesta, A., Ayuela, A., Aranda, M.A.G., 2021. Belite cements and their activation. Cem. Concr. Res. 140, 106319 https://doi.org/10.1016/j.cemconres.2020.106319.

Dilnesa, B.Z., Lothenbach, B., Renaudin, G., Wichsher, A., Kulik, D., 2013. Synthesis and characterization of hydrogarnet Ca3(AlxFe1-x)2(SiO4)y(OH)4(3-y). Cem. Concr. Res. 96–111. https://doi.org/10.1016/j.cemconres.2014.02.001.

Dutch Government, Regeling bodemkwaliteit - Dutch Soil Decree - Appendix A, (2007).

EN, 2002. EN 12457-2:2002 - Characterisation of Waste - Leaching - Compliance Test for Leaching of Granular.

Erdoğan, S.T., Bilginer, B.A., Canbek, O., 2022. Preparation and characterization of magnesium oxalate cement. Eng. Arch. https://doi.org/10.31224/2298.

Gualtieri, A.F., 2000. Accuracy of XRPD QPA using the combined Rietveld ± RIR method research papers. J. Appl. Crystallogr. 33, 267–278. https://doi.org/10.1107/S002188989901643X.

Habert, G., Miller, S.A., John, V.M., Provis, J.L., Favier, A., Horvath, A., Scrivener, K.L., 2020. Environmental impacts and decarbonization strategies in the cement and concrete industries. Nat. Rev. Earth Environ. 1, 559–573. https://doi.org/10.1038/s43017-020-0093-3.

Ihli, J., Wang, Y.W., Cantaert, B., Kim, Y.Y., Green, D.C., Bomans, P.H.H., Sommerdijk, N.A.J.M., Meldrum, F.C., 2015. Precipitation of amorphous calcium oxalate in aqueous solution. Chem. Mater. 27, 3999–4007. https://doi.org/10.1021/acs.chemmater.5b01642.

Iliushchenko, V., Sedla˘, M., 2022. Effect of Alkali Salts on the Hydration Process of Belite Clinker.

IPCC, 2019. Annex I : Glossary. Climate change and Land. IPCC Special Report on Climate Change, Desertification, Land Degradation, Sustainable Land Management, Food Security, and Greenhouse Gas Fluxes in Terrestrial Ecosystems. https://doi.org/10.1017/9781009157988.010.

Jiang, Y., Ling, T., Shi, C., Pan, S., 2018b. Characteristics of steel slags and their use in cement and concrete — a review. Resour. Conserv. Recycl. 136, 187–197. https://doi.org/10.1016/j.resconrec.2018.04.023.

Jiang, Y., Ling, T.C., Shi, C., Pan, S.Y., 2018a. Characteristics of steel slags and their use in cement and concrete—a review. Resour. Conserv. Recycl. 136, 187–197. https://doi.org/10.1016/j.resconrec.2018.04.023.

Kaja, A.M., Delsing, A., Van Der Laan, S.R., Brouwers, H.J.H., Yu, Q., 2021b. Effects of carbonation on the retention of heavy metals in chemically activated BOF slag pastes. Cem. Concr. Res. 148, 106534 https://doi.org/10.1016/j.cemconres.2021.106534.

Kaja, A.M., Schollbach, K., Melzer, S., van der Laan, S.R., Brouwers, H.J.H., Yu, Q., 2021a. Hydration of potassium citrate-activated BOF slag. Cem. Concr. Res. 140, 106291 https://doi.org/10.1016/j.cemconres.2020.106291.

K. Kapetanaki, E. Vazgiouraki, D. Stefanakis, A. Fotiou, TEOS modified with nano-calcium oxalate and PDMS to protect concrete based cultural heritage buildings, 7 (2020) 1–13. doi:10.3389/fmats.2020.00016.

Kindness, A., Macias, A., Glasser, F.P., 1994. Immobilization of Chromium in cement matrices. Waste Manag. 14 (1), 3–11. https://doi.org/10.1016/0956-053X(94)90016-7.

Kloprogge, J.T., 2017. Infrared and Raman Spectroscopy of Minerals and Inorganic Materials, 3rd ed. Elsevier Ltd. https://doi.org/10.1016/B978-0-12-409547-2.12154-7

Lawson-wood, K., Robertson, I., 2016. Study of the decomposition of calcium oxalate monohydrate using a hyphenated thermogravimetric analyser - FT-IR system (TG-IR). Perkin Elmer 1–3. https://www.perkinelmer.com/lab-solutions/resources/docs/APP_Decomposition_CalciumOxalate_Monohydrate(013078_01).pdf%0Ahttps://mondo.su.se/access/content/group/ee616fea-4bdd-47d6-9eb9-1eb4cd1aa4ec/Labcompendium/APP_Decomposition_CalciumOxalate_Monohydr.

C. Li, L. Wang, M. Yuan, H. Xu, J. Dong, A new route for indirect mineralization of carbon dioxide – sodium oxalate as a detergent builder, (2019) 1–9. doi:10.1038/s41598-019-49127-8.

Liu, J., Guo, R., 2018. Applications of Steel Slag Powder and Steel Slag Aggregate in Ultra-High Performance Concrete, 2018.

Lothenbach, B., Scrivener, K., Snellings, R., 2016. A Practical Guide to Microstructural Analysis of Cementitious Materials.

Mancini, A., Wieland, E., Geng, G., Dähn, R., Skibsted, J., Wehrli, B., Lothenbach, B., 2019. Fe(III) uptake by calcium silicate hydrates. Appl. Geochem., 104460 https://doi.org/10.1016/j.apgeochem.2019.104460.

Manuel, D., Cobos, G., 2018. The Role of Superplasticizers and Their Degradation Products On Radionuclide Mobility. Universitat Politècnica de Catalunya Barcelonatech.

Miller, S.A., John, V.M., Pacca, S.A., Horvath, A., 2018. Carbon dioxide reduction potential in the global cement industry by 2050. Cem. Concr. Res. 114, 115–124. https://doi.org/10.1016/j.cemconres.2017.08.026.

Monteiro, P.J.M., Miller, S.A., Horvath, A., 2017. Produce and use with care - towards sustainable concrete. Nat. Mater. 16, 698–699. https://doi.org/10.1038/nmat4930.

Moulin, I., Rose, J., Stone, W., Bottero, J., 2000. Waste Materials in Construction, pp. 269–280.

Nicoleau, L., Nonat, A., Perrey, D., 2013. The di- and tricalcium silicate dissolutions. Cem. Concr. Res. 47, 14–30. https://doi.org/10.1016/j.cemconres.2013.01.017.

Osmolovskaya, N., Dung, V.V., Kuchaeva, L., 2018. The role of organic acids in heavy metal tolerance in plants. Biol. Commun. 63, 9–16. https://doi.org/10.21638/spbu03.2018.103.

Pan, S.Y., Chung, T.C., Ho, C.C., Hou, C.J., Chen, Y.H., Chiang, P.C., 2017. CO2 Mineralization and utilization using steel slag for establishing a waste-to-resource supply chain. Sci. Rep. 7, 1–11. https://doi.org/10.1038/s41598-017-17648-9.

Paris, A.R., Bocarsly, A.B., 2019. High-efficiency conversion of CO_2 to oxalate in water is possible using a Cr-Ga oxide electrocatalyst. ACS Catal. 9, 2324–2333. https://doi.org/10.1021/acscatal.8b04327.

Petter, J., 2019. Vanadium geochemistry in the biogeosphere – speciation, solid-solution interactions, and ecotoxicity. Appl. Geochem. 102, 1–25. https://doi.org/10.1016/j.apgeochem.2018.12.027.

Post, J., Bish, D., 1989. Rietveld refinement of crystal structures using powder X-ray diffraction data. Mineral. Soc. Am. 20, 277–308.

Provis, J.L., 2018. Alkali-activated materials. Cem. Concr. Res. 114, 40–48. https://doi.org/10.1016/j.cemconres.2017.02.009.

Provis, J.L., van Deventer, J.S.J., 2009. Geopolymers - Structure, Processing, Properties and Industrial Applications. Woodhead Publishing Limited, Cambridge.

Ramachandran, V.S., 1972. Elucidation of the role of chemical admixtures in hydrating cements by DTA technique. Thermochim. Acta. 4.

Ruiz-Agudo, E., Burgos-Cara, A., Ruiz-Agudo, C., Ibañez-Velasco, A., Cölfen, H., Rodriguez-Navarro, C., 2017. A non-classical view on calcium oxalate precipitation and the role of citrate. Nat. Commun. 8 https://doi.org/10.1038/s41467-017-00756-5.

Salman, M., Cizer, Ö., Pontikes, Y., Snellings, R., Vandewalle, L., Blanpain, B., Van Balen, K., 2015. Cementitious binders from activated stainless steel refining slag and the effect of alkali solutions. J. Hazard. Mater. 286, 211–219. https://doi.org/10.1016/j.jhazmat.2014.12.046.

Santos, W.F., Schollbach, K., Melzer, S., van der Laan, S.R., Brouwers, H.J.H., 2023. Quantitative analysis and phase assemblage of basic oxygen furnace slag hydration. J. Hazard. Mater. 450, 131029 https://doi.org/10.1016/j.jhazmat.2023.131029.

Schuler, E., Morana, M., Shiju, N.R., Gruter, G.-J.M., 2022. A new way to make oxalic acid from CO_2 and alkali formates: using the active carbonite intermediate. Sustain. Chem. Clim. Action. 1, 100001 https://doi.org/10.1016/j.scca.2022.100001.

Scrivener, K.L., John, V.M., Gartner, E.M., 2018. Eco-efficient cements: potential economically viable solutions for a low-CO2 cement-based materials industry. Cem. Concr. Res. 114, 2–26. https://doi.org/10.1016/J.CEMCONRES.2018.03.015.

Shi, C., 2004. Steel Slag — Its Production, Processing, Characteristics, and Cementitious Properties, pp. 230–236.

Shi, C., Qian, J., 2000. High performance cementing materials from industrial slags - a review. Resour. Conserv. Recycl. 29, 195–207. https://doi.org/10.1016/S0921-3449(99)00060-9.

N.K. Singh, P.C. Mishra, V.K. Singh, K.K. Narang, Effects of hydroxyethyl cellulose and oxalic acid on the properties of cement, 33 (2003) 1319–1329. doi:10.1016/S0008-8846(03)00060-7.

Smillie, S., Glasser, F.P., 1999. Reaction of EDTA, Oxalic Acid and Citric Acid with Portland Cement, pp. 97–101.

Snellings, R., Chwast, J., Cizer, Ö., De Belie, N., Dhandapani, Y., Durdzinski, P., Elsen, J., Haufe, J., Hooton, D., Patapy, C., Santhanam, M., Scrivener, K., Snoeck, D., Steger, L., Tongbo, S., Vollpracht, A., Winnefeld, F., Lothenbach, B., 2018. RILEM TC-238 SCM recommendation on hydration stoppage by solvent exchange for the study of hydrate assemblages. Mater. Struct. Constr. 51 https://doi.org/10.1617/s11527-018-1298-5.

Song, Q., Guo, M., Wang, L., Ling, T., 2021. Use of steel slag as sustainable construction materials : a review of accelerated carbonation treatment. Resour. Conserv. Recycl. 173, 105740 https://doi.org/10.1016/j.resconrec.2021.105740.

Spence, R., Shi, C., 2005. Stabilization and Solidification of Hazardous, Radioactive, and Mixed Wastes. CRC Press. CRC Press.

Taylor, H.F.W., 1997. Cement chemistry. Cem. Chem. https://doi.org/10.1680/cc.25929.

Toby, B.H., 2006. R Factors in Rietveld Analysis : How Good is Good Enough ?, pp. 67–70. https://doi.org/10.1154/1.2179804.

van Hoek, C., Small, J., van der Laan, S., 2016. Large-area phase mapping using PhAse Recognition and Characterization (PARC) software. Micros. Today. 24, 12–21. https://doi.org/10.1017/S1551929516000572.

van Zomeren, A., van der Laan, S.R., Kobesen, H.B.A., Huijgen, W.J.J., Comans, R.N.J., 2011. Changes in mineralogical and leaching properties of converter steel slag resulting from accelerated carbonation at low CO2 pressure. Waste Manag. 31, 2236–2244. https://doi.org/10.1016/j.wasman.2011.05.022.

Wang, G., Wang, Y., Gao, Z., 2010. Use of steel slag as a granular material: volume expansion prediction and usability criteria. J. Hazard. Mater. 184, 555–560. https://doi.org/10.1016/J.JHAZMAT.2010.08.071.

Wang, Q., Yang, J., Yan, P., 2012. Influence of initial alkalinity on the hydration of steel slag. Sci. China Technol. Sci. 55, 3378–3387. https://doi.org/10.1007/s11431-012-4830-9.

Wang, X., Lu, X., Turvey, C.C., Dipple, G.M., Ni, W., 2022. Evaluation of the carbon sequestration potential of steel slag in China based on theoretical and experimental labile Ca. Resour. Conserv. Recycl. 186, 106590 https://doi.org/10.1016/j.resconrec.2022.106590.

World Steel Association, World Steel Figures, World Steel Assoc. (2022). https://worldsteel.org/steel-topics/statistics/world-steel-in-figures-2022/.

H. Yi, G. Xu, H. Cheng, J. Wang, Y. Wan, H. Chen, An overview of utilization of steel slag, 16 (2012) 791–801. doi:10.1016/j.proenv.2012.10.108.

Zepper, J.C.O., van der Laan, S.R., Schollbach, K., Brouwers, H.J.H., 2023. Reactivity of BOF slag under autoclaving conditions. Constr. Build. Mater. 364, 129957 https://doi.org/10.1016/j.conbuildmat.2022.129957.

Zha, J., Gu, Y., Wei, S., Han, H., Wang, F., Ma, Q., 2022. Facile two-step deposition of calcium oxalate film on dolomite to improve acid rain resistance. Crystals 12, 734. https://doi.org/10.3390/cryst12050734.

Zhang, M., Zhao, M., Peng, J., Liu, X., Huang, Q., Zhao, L., 2021. Improvement on corrosion resistance of gypsum for ceramics molding with soluble salts. J. Build. Eng. 35, 102064 https://doi.org/10.1016/j.jobe.2020.102064.

Zhao, J., Yan, P., Wang, D., 2017. Research on mineral characteristics of converter steel slag and its comprehensive utilization of internal and external recycle. J. Clean. Prod. 156, 50–61. https://doi.org/10.1016/j.jclepro.2017.04.029.